RAA 2014 Vol. **14** No. **11**, 1447–1457 doi: 10.1088/1674–4527/14/11/008
http://www.raa-journal.org *http://www.iop.org/journals/raa*

Research in Astronomy and Astrophysics

Precise determination of fundamental parameters of six exoplanet host stars and their planets *

Kang Liu[1], Shao-Lan Bi[1], Tan-Da Li[1,2], Zhi-E Liu[1], Zhi-Jia Tian[1] and Zhi-Shuai Ge[1]

[1] Department of Astronomy, Beijing Normal University, Beijing 100875, China; *liukang@mail.bnu.edu.cn; bisl@bnu.edu.cn*
[2] National Astronomical Observatories, Chinese Academy of Sciences, Beijing 100012, China

Received 2014 April 9; accepted 2014 April 25

Abstract The aim of this paper is to determinate the fundamental parameters of six exoplanet host (EH) stars and their planets. Because techniques for detecting exoplanets yield properties of the planet only as a function of the properties of the host star, we must accurately determine the parameters of the EH stars first. For this reason, we constructed a grid of stellar models including diffusion and rotation-induced extra-mixing with given ranges of input parameters (i.e. mass, metallicity and initial rotation rate). In addition to the commonly used observational constraints such as the effective temperature $T_{\rm eff}$, luminosity L and metallicity [Fe/H], we added two observational constraints, the lithium abundance $\log N$ (Li) and the rotational period $P_{\rm rot}$. These two additional observed parameters can set further constraints on the model due to their correlations with mass, age and other stellar properties. Hence, our estimations of the fundamental parameters for these EH stars and their planets have a higher precision than previous works. Therefore, the combination of rotational period and lithium helps us to obtain more accurate parameters for stars, leading to an improvement in knowledge about the physical state of EH stars and their planets.

Key words: stars: fundamental parameters – stars: abundances – stars: evolution – stars: rotation – stars: planetary systems

1 INTRODUCTION

During the past two decades, thousands of identifiable planets outside the solar system have already been spotted (e.g. Vogt et al. 2000; Pietrukowicz et al. 2010; Moutou et al. 2011; Ofir & Dreizler 2013; Rowe et al. 2014). An overwhelming majority of them have been discovered using indirect methods, i.e., radial velocity (RV) and photometric transits. This is due to the fact that planets are non-luminous bodies, which merely reflect light from their parent star. From a distance of a few parsecs, a planet is like a small "undetectable" speckle in the stellar image. But a planet can cause dynamical perturbations onto its parent star, providing the possibility to detect it by indirect means. As a consequence, this makes the characteristic parameters of an exoplanet depend strongly on the characteristic parameters of the host star. Hence, it is of great significance to obtain as accurate

* Supported by the National Natural Science Foundation of China.

values as possible for masses and radii of host stars to study their associated exoplanets (e.g. Seager & Mallén-Ornelas 2003; Santos 2008; Winn 2010).

The most commonly used method for determination of the stellar properties is to fit the parameters of theoretical models with the observational constraints, e.g. effective temperature $T_{\rm eff}$ and luminosity $L/L_{\odot}$. However, this method generally makes it difficult to obtain sets of complete stellar atmospheric parameters. There are a few free parameters in stellar structure and evolution models, which introduce more uncertainties into the observations and result in insufficient estimation of the stellar properties (Bi et al. 2008).

Nevertheless, the abundance of lithium in stellar photospheres is usually used to study various processes, from Big Bang nucleosynthesis to the formation and evolution of planetary systems (e.g., Meléndez et al. 2010; Santos et al. 2010). Lithium is readily destroyed in stellar interiors at a comparatively low temperature ($\sim 2.5 \times 10^6$ K), therefore, in solar-like stars, the surface lithium abundance has been treated as an extremely sensitive diagnostic for stellar structure and evolution. Additionally, the evolution of lithium abundance during pre-main sequence (pre-MS) and MS phases has strong correlations with several properties of a star, i.e. metallicity, mass, age and rotational history. Meanwhile, due to the total angular momentum loss induced by magnetic braking, the rotational period of solar-like stars decreases with age during the main sequence. The rate of angular momentum loss is related to the stellar mass, radius and rotational rate. Accordingly, by combining a non-standard stellar model which includes the process of extra-mixing with an accurate measurement of the lithium abundance and rotational period, we can obtain a more precise estimation for fundamental parameters of EH stars and their planets (Do Nascimento et al. 2009; Castro et al. 2011; Li et al. 2012).

In this work, we computed evolutionary models including rotation-induced element mixing and microscopic diffusion. We used three common observation constraints ($T_{\rm eff}$, $L/L_{\odot}$ and [Fe/H]) and two additional observation constraints (lithium abundance $\log N$ (Li) and rotational period $P_{\rm rot}$) as restrictions on stellar models, aiming to accurately calculate the stellar parameters. We assumed that the depletion of lithium happens at the pre-MS stage and the lithium evolves differently with different initial rotational rates.

The observed data of the six EH stars and their planets are summarized in Section 2. The computational method and the details of our evolutionary models are described in Section 3. In Section 4, we present our modeling results and compare them with previous studies. We end with a discussion and the conclusions in Section 5.

2 THE SELECTION OF OUR SAMPLE OF STARS

2.1 EH Stars

The sample of stars used for our modeling are six solar-analog stars with observed lithium abundances and rotational periods, and their planets have been detected by using RV. The detections of lithium abundances and rotational periods mean it is possible to obtain precise estimations of stellar parameters, especially the masses and radii, which are useful for us to determine the properties of their planets.

We summarized the observed data about the EH stars that were used for our theoretical calculations in Table 1. The atmospheric features $T_{\rm eff}$, L and [Fe/H] were collected from Valenti & Fischer (2005), Ghezzi et al. (2010a), Israelian et al. (2004) and Baumann et al. (2010). We adopted the lithium abundance $\log N$(Li) from the observations of Ghezzi et al. (2010b), Israelian et al. (2004) and Baumann et al. (2010). The rotational period $P_{\rm rot}$ we used was determined by Wright et al. (2004) from the California and Carnegie Planet Search Program with the HIRES spectrometer at the Keck Observatory. The average values of these observations were adopted in the following study.

The spectra of Valenti & Fischer (2005) were obtained with the HIRES spectrograph mounted on the 10-m telescope at the Keck Observatory (Vogt et al. 1994), the UCLES spectrograph mounted

Table 1 Main Characteristics of Six EH Stars

HIP	HD	$T_{\rm eff}$ (K)	$\log(L/L_{\odot})$	[Fe/H]	$\log N$ (Li) (dex)	$P_{\rm rot}$	Ref
9683	12661	5743±44	0.093±0.063	0.36±0.03	...	...	[1]
		5785±50	0.033±0.063	0.37±0.03	1.10±0.60	...	[2]
		5715±70	...	0.36	...	...	[3]
		...	...	...	...	35±2.1	[5]
		5748±70	0.063±0.063	0.36±0.03	1.10±0.60	35±2.1	[6]
33212	50554	5929±44	0.167±0.063	–0.07±0.03	...	...	[1]
		5982±26	0.119±0.062	–0.07±0.02	2.40±.011	...	[2]
		6050±70	...	0.02	2.59	...	[3]
		...	...	...	...	16±1.0	[5]
		5987±70	0.143±0.063	–0.04±0.03	2.50±0.11	16±1.0	[6]
47007	82943	5997±44	0.169±0.047	0.27±0.03	...	...	[1]
		6011±36	0.152±0.061	0.28±0.03	2.47±0.10	...	[2]
		6025±70	...	0.33	2.52	...	[3]
		...	...	...	...	20±1.2	[5]
		6011±70	0.161±0.061	0.29±0.03	2.50±0.10	20±1.2	[6]
50473	89307	5898±44	0.096±0.062	–0.16±0.03	...	...	[1]
		5914±25	0.130±0.063	–0.18±0.02	2.18±0.11	...	[2]
		...	...	...	...	18±1.1	[5]
		5906±44	0.113±0.063	–0.17±0.03	2.18±0.11	18±1.1	[6]
59610	106252	5870±44	0.107±0.069	–0.08±0.03	...	...	[1]
		5923±38	0.108±0.063	–0.05±0.03	1.69±0.13	...	[2]
		5890±70	...	–0.01	1.65	...	[3]
		5899±62	...	–0.034±0.041	1.71±0.04	...	[4]
		...	...	...	...	23±1.4	[5]
		5896±70	0.108±0.069	–0.04±0.04	1.68±0.13	23±1.4	[6]
77740	141937	5847±44	0.070±0.073	0.13±0.03	...	...	[1]
		5842±36	-0.026±0.067	0.10±0.03	2.26±0.11	...	[2]
		5925±70	...	0.11	2.48	...	[3]
		5900±19	...	0.125±0.030	2.36±0.02	...	[4]
		...	...	...	...	21±1.3	[5]
		5879±70	0.022±0.073	0.12±0.03	2.37±0.11	21±1.3	[6]

Reference: [1] Valenti & Fischer (2005); [2] Ghezzi et al. (2010a) and Ghezzi et al. (2010b); [3] Israelian et al. (2004); [4] Baumann et al. (2010); [5] Wright et al. (2004); [6] Mean value.

on the 4-m Anglo-Australian Telescope at the Siding Spring Observatory (Diego et al. 1990), and the Hamilton echelle spectrometer at the Lick Observatory (Vogt 1987). The spectra of Ghezzi et al. (2010a,b) were obtained with the FEROS spectrograph mounted on the MPG/ESO 2.20-m telescope at La Silla (Kaufer et al. 1999). The observations from Israelian et al. (2004) were carried out using the UES/4.2-m William Hershel Telescope, the SARG/3.5-m TNG at La Palma, the FEROS/1.52-m ESO and the CORALIE/1.2-m Euler Swiss at La Silla. Stars from Baumann et al. (2010) were observed with the RGT spectrograph mounted on the 2.7-m Harlan Smith telescope at McDonald Observatory, the MIKE spectrograph mounted on the 6.5-m Magellan Clay telescope at Las Campanas Observatory and the HARPS spectrograph mounted on the 3.6-m ESO telescope at La Silla Observatory.

2.2 Exoplanets

We list the planetary orbital parameters that were obtained by RV measurements in Table 2. Two of these systems are found to be multi-planetary cases. HD 12661 and HD 82943 host two and three

Table 2 Main Characteristics of Exoplanets

Planet	P (d)	e	K_1 (m s^{-1})	Ref
HD 12661b	262.709 ± 0.083	0.3768 ± 0.0077	73.56 ± 0.56	[1]
HD 12661c	1708.0 ± 14.0	0.031 ± 0.022	30.41 ± 0.62	[1]
HD 50554b	1293.0 ± 37.0	0.501 ± 0.030	104 ± 5	[2]
HD 82943b	442.4 ± 3.1	0.203 ± 0.052	39.8 ± 1.3	[3]
HD 82943c	219.3 ± 0.8	0.425 ± 0.018	54.4 ± 2.0	[3]
HD 82943d	1072 ± 13	0 ± 0	5.39 ± 0.57	[4]
HD 89307b	2199 ± 61	0.25 ± 0.09	32.4 ± 4.5	[5]
HD 106252b	1600.0 ± 18.0	0.471 ± 0.028	147 ± 4	[2]
HD 141937b	653.22 ± 1.21	0.41 ± 0.01	234.5 ± 6.4	[6]

Reference: [1] Wright et al. (2009); [2] Perrier et al. (2003); [3] Tan et al. (2013); [4] Baluev & Beaugé (2014); [5] Boisse et al. (2012); [6] Udry et al. (2002).

planets, respectively. Orbital period P, eccentricity e and semi-amplitude K_1 (the velocity wobble) are given here; more details about parameters describing the planetary motion, such as the periastron passage time T and the angle between the periastron and the line-of-nodes ω, can be found in the related literature.

The RV data were acquired from the HIRES spectrograph (HD 12661 and HD 82943) mounted on the 10-m Keck-1 telescope at Keck Observatory (Vogt et al. 1994), the ELODIE echelle spectrograph (HD 50554 and HD 106252) and the SOPHIE spectrograph (HD 89307) mounted on the Cassegrain focus of the 1.93-m telescope at the Haute-Provence Observatory (Baranne et al. 1996), and the CORALIE echelle spectrograph (HD 141937) mounted on the 1.2-m Euler Swiss telescope at La Silla Observatory (Queloz et al. 2000; Udry et al. 2000).

3 STELLAR MODELS

3.1 Input Physics

To estimate the parameters of stars in the sample, a grid calculation was carried out based on a stellar evolutionary model named the Yale Rotating Stellar Evolution Code (YREC) (Pinsonneault et al. 1990, 1992; Demarque et al. 2008), which includes diffusion, angular momentum loss, angular momentum transport and rotation induced mixing of elements. Detailed descriptions of the model can be found in Guenther et al. (1992), Chaboyer et al. (1995) and Li et al. (2003). The calculations were carried out with the up-to-date OPAL equation-of-state tables EOS2005 (Rogers & Nayfonov 2002). The solar mixture of GS98 (Grevesse & Sauval 1998) ($Z_\odot$ = 0.0170 and $(Z/X)_\odot$ = 0.0230) was adopted and hence the opacities were generated with the composition of GS98 (Grevesse & Sauval 1998) and supplemented by low-temperature opacities from Ferguson et al. (2005). The atmosphere of the model follows the Eddington $T-\tau$ relation. We used NACRE reaction rates (Angulo et al. 1999) for nuclear reaction and the mixing length theory (Böhm-Vitense 1958) for convection. Following the formulation of Thoul et al. (1994), the gravitational settling of helium and heavy elements is considered in the stellar model.

When rotation is taken into account, the characteristics of a model depend on six parameters: mass M, age t, mixing-length parameter $\alpha \equiv l/Hp$, two parameters ($X_{\rm ini}$ and $Z_{\rm ini}$) that describe the initial chemical composition of a star, and rotational period $P_{\rm rot}$. To reproduce the evolution of lithium, evolutions of stars during the pre-MS stage are considered and hence we selected the initial model for each calculation on the Hayashi track. All of the models evolved to exhaust their supply of the hydrogen in the core. Initial helium abundance ($Y_{\rm ini}$ = 0.275) and the mixing-length parameter (α = 1.75) were regarded as constants in the grid computation.

The ranges of the variable parameters in the grid calculation and their step sizes are shown in Table 3. According to the effective temperatures of the sample stars, we set the range of mass from

Table 3 Input Parameters for Theoretical Calculation

Variate	Min	Max	δ^{a}
$M(M_{\odot})$	0.90	1.10	0.01
Z	0.010	0.040	0.001
$V_{\rm ZAMS}$ (km s^{-1})	20	70	10

Notes: [a] The value of δ represents the increment between the minimum and maximum values.

0.90 to 1.10 $M_{\odot}$ with a grid size of 0.01 $M_{\odot}$. The range of mass fraction of all heavy elements $Z_{\rm ini}$, which was derived from $Z_{\odot}$ and the observed [Fe/H], is from 0.010–0.040 dex with a grid size of 0.001 dex. Although the initial models were selected to be on the Hayashi track, we used the rotational rates at zero age main sequence ($V_{\rm ZAMS}$) to represent the rotational conditions for better understanding. The range of $V_{\rm ZAMS}$ is from 20 to 70 km s^{-1}, in steps of 10 km s^{-1}.

3.2 Angular Momentum Loss

The braking law of Kawaler (1988) is adopted as the angular momentum loss equation

$$\frac{dJ}{dt} = \begin{cases} -K\Omega^3(R/R_{\odot})^{1/2}(M/M_{\odot})^{-1/2}(\Omega \leq \Omega_{\rm sat})\,, \\ -K\Omega{\Omega_{\rm sat}}^2(R/R_{\odot})^{1/2}(M/M_{\odot})^{-1/2}(\Omega > \Omega_{\rm sat}), \end{cases} \tag{1}$$

where the parameter K is constant for all stars, and is associated with the magnetic field intensity. $\Omega_{\rm sat}$ is the angular velocity of the surface when magnetic saturation occurs in the star. Both K and $\Omega_{\rm sat}$ are free parameters and we follow Bouvier et al. (1997) by setting $K = 2.0 \times 10^{47}$ g cm^2 s and $\Omega_{\rm sat} = 14\,\Omega_{\odot}$.

3.3 Extra-mixing in the Radiative Region

Besides the microscopic diffusion of elements, which we have mentioned above, angular momentum transport and element mixing caused by rotation are taken into account in radiative regions. These processes can be described as a coupled set of diffusion equations (Chaboyer et al. 1995)

$$\rho r^2 \frac{I}{M}\frac{d\Omega}{dt} = \frac{d}{dr}\left(\rho r^2 \frac{I}{M} D_{\rm rot}\frac{d\Omega}{dt}\right)\,, \tag{2}$$

$$\rho r^2 \frac{dX_i}{dt} = \frac{d}{dr}\left[\rho r^2 D_{m,1} X_i + \rho r^2 (D_{m,2} + f_c D_{\rm rot})\frac{dX_i}{dt}\right]\,, \tag{3}$$

where Ω is the angular velocity, X_i is the mass fraction of chemical species i and I/M is the moment of inertia per unit mass. $D_{m,1}$ and $D_{m,2}$ are the microscopic diffusion coefficients. $D_{\rm rot}$ is the diffusion coefficient caused by rotation-induced mixing. More details about these diffusion coefficients were given by Chaboyer et al. (1995). The tunable parameter f_c was used to alter the effects of rotation-induced element mixing. It was determined by observations, that is, the depletion of lithium in our solar model must fit the observed depletion in the Sun (Chaboyer et al. 1995).

4 RESULTS

4.1 Stellar Parameters

We calculated a series of evolutionary models in estimated M and $Z_{\rm ini}$ ranges to reproduce the observational constraints of these six EH stars. As shown in Figure 1, evolutionary tracks for each

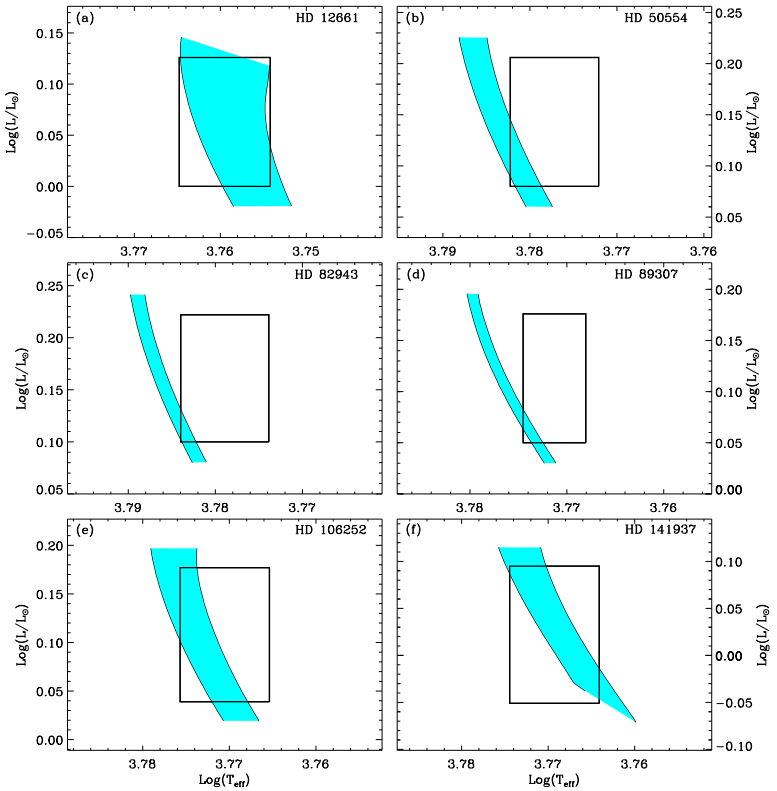

Fig. 1 Evolutionary tracks of HD 12661, HD 50554, HD 82943, HD 89307, HD 106252 and HD 141937 in the H-R diagram constrained by (a) $T_{\rm eff}$ + L + [Fe/H]; (b) $T_{\rm eff}$ + L + [Fe/H] + $\log N$(Li); (c) $T_{\rm eff}$ + L + [Fe/H] + $\log N$(Li) + $P_{\rm rot}$.

star are plotted to conform with observational constraints. For the sake of simplicity, the case of star HD 12661 is taken as an example.

First of all, three classical observed features, the effective temperature $T_{\rm eff}$, luminosity L and metallicity [Fe/H], were considered and 157 tracks were found fitting these three observational constraints. The mass and age of HD 12661 provided by the models are 1.02 $\pm$ 0.03 $M_{\odot}$ and 6.76 $\pm$ 4.31 Gyr respectively.

Secondly, lithium abundance was taken into account. Lithium is the most important element since it is readily burned in stellar interiors. The abundance of lithium indicates the extent of element mixing in stars. In addition, the depletion of lithium depends strongly on the mass and age of the star (Do Nascimento et al. 2009; Li et al. 2012). In this step, there are only 76 evolutionary tracks which fit four observational constraints, including lithium abundance $\log N$ (Li), and we estimate the mass and age of the star HD 12661 to be 1.02 ± 0.02 $M_{\odot}$ and 5.56 ± 3.01 Gyr respectively. Additionally, lithium abundance narrows the ranges of input parameters, thus the possible position of the star in the H-R diagram is restricted to a smaller field than what has been obtained above.

Finally, after adding the rotational period to our models as a constraint, only 30 evolutionary tracks are found fitting the observed $P_{\rm rot}$. The range of $V_{\rm ZAMS}$ is significantly reduced to 30–40 km s^{-1}. In the same way as lithium abundance, the ranges of input parameters for the stellar

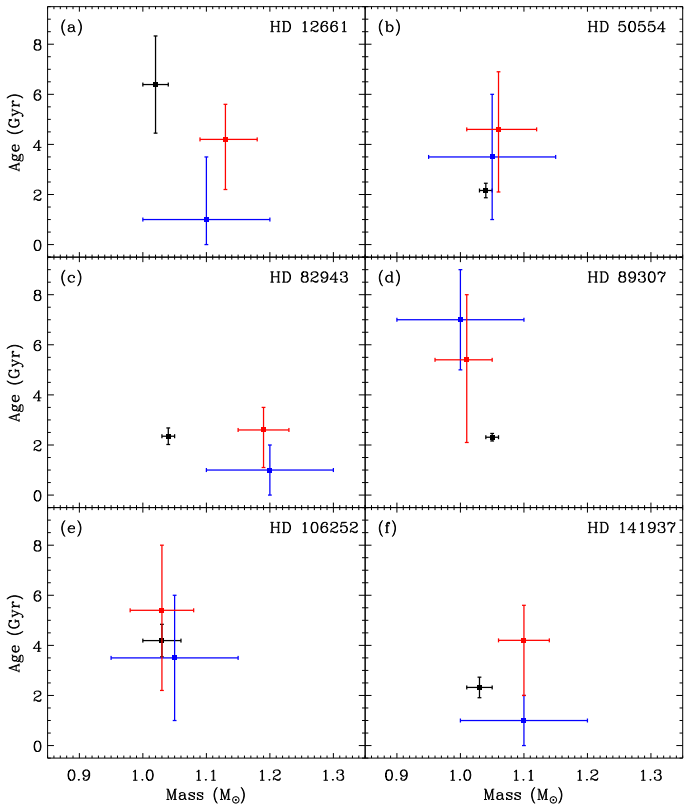

Fig. 2 Comparisons between masses and ages determined by our model (*black* error bars) and estimates of previous studies for all six EH stars. The red and blue error bars represent the results of Valenti & Fischer (2005) and Ghezzi et al. (2010a), respectively.

models are also reduced by the rotational period, and hence it sets a further constraint on the possible position of the star in the H-R diagram, as shown in Figure 1(a). The rotational period $P_{\rm rot}$ helps us determinate the mass and age of HD 12661 even more precisely, which are $1.02 \pm 0.02\ M_{\odot}$ and 6.39 ± 1.94 Gyr respectively.

The same method was adopted for all the other EH stars; we plotted their evolutionary tracks in Figure 1, where each line illustrates a given star as labeled. Comparing the situation of star HD 12661 with the others, we find that this star occupies a larger area in the H-R diagram than the other five stars in Figure 1; this is due to a large error in the abundance of lithium for HD 12661.

4.2 Comparison with Previous Results

These six EH stars were previously studied by several researchers; the methods and estimates of two of them can be seen in Table 4. Ghezzi et al. (2010a) and Valenti & Fischer (2005) observed these stars and provided their masses, radii and ages through different methods. We compare their results obtained by interpolating isochrones with ours in the following paragraphs. The comparisons of masses and ages of these six EH stars are plotted in Figure 2.

For the six EH stars, the results of Ghezzi et al. (2010a) are shown, given the error in mass is $\sim 0.10\,M_{\odot}$ and the error in age is ~ 2.0 Gyr. The mass determinations of Valenti & Fischer (2005) were close to those of Ghezzi et al. (2010a) but with higher precision, i.e., $\Delta M \sim 0.05\,M_{\odot}$. Our mass estimations of HD 12661, HD 50554, HD 82943, HD 89307, HD 106252 and HD 141937 are 1.02 ± 0.02, 1.04 ± 0.01, 1.04 ± 0.01, 1.05 ± 0.01, 1.03 ± 0.03 and $1.03 \pm 0.02\,M_{\odot}$, respectively, most of which are less massive than what have been obtained by Ghezzi et al. (2010a) and Valenti & Fischer (2005). This result is due to the element transport, which is caused by the interaction between diffusion and rotation-induced mixing in the stellar radiative region (Chaboyer et al. 1995; Eggenberger et al. 2010). The process of element transport changes the chemical composition of the external layers and hence causes the evolutionary tracks to shift toward the hot side of the H-R diagram. Thus, when the observed effective temperature is given, the rotational model tends to provide a less massive result than those obtained by the standard model. The precision of our mass determinations is the best of the three, which is $0.01 \sim 0.03$.

The ages of these six EH stars provided by Valenti & Fischer (2005) are mostly older than those of Ghezzi et al. (2010a), with a similar accuracy, i.e., $\Delta t \sim 2.0$ Gyr. Our age determinations generally agree within the errors of previous works, and are much more accurate ($\Delta t \sim 0.5$ Gyr) than what is determined by interpolating isochrones. (see Table 4). Moreover, combining the rotational periods listed in Table 1 with the ages obtained by us, we found that there is a positive correlation between them.

This result is reasonable, because the depletion of lithium is a function of stellar mass, age, rotational rates and metallicity, while the rotational period increases with age during the main sequence. Therefore, these two additional observational constraints can effectively restrict the ranges of the input parameters and improve the precision of the stellar model.

4.3 Planetary Parameters

For a given planetary system with known orbital parameters, we can calculate the mass function (Santos 2008)

$$f(m) = \frac{(M_2 \sin i)^3}{(M_1 + M_2)^2} = 1.036 \times 10^{-7} K_1^3 (1 - e^2)^{(3/2)} P, \tag{4}$$

where M_1 and M_2 are the masses of the star and planet respectively, i is the inclination of the line of sight with respect to the orbital axis, K_1 is the semi-amplitude of the RV of the star with mass M_1, e is the orbital eccentricity and P is the orbital period.

Furthermore, we know from Kepler's third law

$$\frac{a^3}{P^2} = \frac{G(M_1 + M_2)}{4\pi^2}, \tag{5}$$

where *a* is the orbital semimajor axis and *G* is the universal gravitational constant.

From Equations (4) and (5), and the combined stellar masses determined in the previous section, the minimum masses $M_2 \sin i$ and orbital semimajor axes a of planets can be obtained, as shown in Table 5. It should be noted that the uncertainty in our estimation consists of two parts. One is associated with the observation, such as the errors in P, e and K_1 (listed in Table 2). The other is produced by the model, specifically, the error in stellar mass. We summarize the two parts of the uncertainty separately in Table 5. Compared with the results of previous studies, our determinations are more accurate, whether including the errors in observations or not.

Batalha et al. (2013) pointed out that a $0.1\,M_{\odot}$ companion would induce a systematic error of approximately 2%. Correspondingly, the accuracy and precision of the parameters of the EH star will have a huge impact on our estimates of the properties of planets. Therefore, accurate knowledge about the EH star is extremely important for the study of exoplanets.

Table 4 Stellar Parameters and Comparison with Previous Studies

Star	M ($M_\odot$)	t (Gyr)	R ($R_\odot$)	Method	Ref
HD 12661	0.96±0.47	...	1.04±0.08	Spectroscopic	[1]
	1.10±0.10	$1.0^{+2.5}_{-1.0}$	...	Isochrones	[1]
	1.22±0.18	...	1.124±0.037	Spectroscopic	[2]
	$1.13^{+0.05}_{-0.04}$	$4.2^{+1.4}_{-2.0}$	...	Isochrones	[2]
	1.02±0.02	6.39±1.94	1.11±0.08	This work	
HD 50554	0.81±0.39	...	1.07±0.08	Spectroscopic	[1]
	1.05±0.10	$3.5^{+2.5}_{-2.5}$	...	Isochrones	[1]
	0.93±0.14	...	1.149±0.039	Spectroscopic	[2]
	$1.06^{+0.06}_{-0.05}$	$4.6^{+2.3}_{-2.5}$	...	Isochrones	[2]
	1.04±0.01	2.16±0.29	1.02±0.02	This work	
HD 82943	1.03±0.50	...	1.10±0.09	Spectroscopic	[1]
	1.20±0.10	$1.0^{+1.0}_{-1.0}$	...	Isochrones	[1]
	1.22±0.17	...	1.125±0.029	Spectroscopic	[2]
	$1.19^{+0.04}_{-0.04}$	$2.6^{+0.9}_{-1.5}$	...	Isochrones	[2]
	1.04±0.01	2.35±0.33	1.03±0.02	This work	
HD 89307	0.85±0.41	...	1.11±0.09	Spectroscopic	[1]
	1.00±0.10	$7.0^{+2.0}_{-2.0}$	...	Isochrones	[1]
	0.91±0.13	...	1.069±0.035	Spectroscopic	[2]
	$1.01^{+0.04}_{-0.05}$	$5.4^{+2.6}_{-3.3}$	...	Isochrones	[2]
	1.05±0.01	2.31±0.15	1.01±0.01	This work	
HD 106252	1.16±0.57	...	1.08±0.09	Spectroscopic	[1]
	1.05±0.10	$3.5^{+2.5}_{-2.5}$	...	Isochrones	[1]
	1.01±0.15	...	1.093±0.040	Spectroscopic	[2]
	$1.03^{+0.05}_{-0.05}$	$5.4^{+2.6}_{-3.2}$	...	Isochrones	[2]
	1.03±0.03	4.19±0.65	1.05±0.01	This work	
HD 141937	0.58±0.28	...	0.95±0.08	Spectroscopic	[1]
	1.10±0.10	$1.0^{+1.0}_{-1.0}$	...	Isochrones	[1]
	1.07±0.13	...	1.056±0.039	Spectroscopic	[2]
	$1.10^{+0.04}_{-0.04}$	$4.2^{+1.4}_{-2.2}$	...	Isochrones	[2]
	1.03±0.02	2.32±0.41	0.99±0.06	This work	

Reference: [1] Ghezzi et al. (2010a); [2] Valenti & Fischer (2005).

Table 5 Planetary Parameters and Comparison with Previous Studies

Planet	Previous Studies			This Work					
	$M \sin i$ ($M_{\rm Jup}$)	a (AU)	Ref	$M \sin i$ ($M_{\rm Jup}$)	$\delta_M^{\rm obs}$ ($M_{\rm Jup}$)	$\delta_M^{\rm theo}$ ($M_{\rm Jup}$)	a (AU)	$\delta_a^{\rm obs}$ (AU)	$\delta_a^{\rm theo}$ (AU)
HD 12661b	2.30 ± 0.19	0.831 ± 0.048	[1]	2.176	0.024	0.028	0.8079	0.0001	0.0052
HD 12661c	1.92 ± 0.16	2.90 ± 0.17	[1]	1.812	0.042	0.023	2.8145	0.0153	0.0182
HD 50554b	5.16	2.41	[2]	4.954	0.388	0.031	2.3530	0.0446	0.0075
HD 82943b	1.59	1.1866	[3]	1.500	0.067	0.009	1.1510	0.0053	0.0036
HD 82943c	1.58	0.7423	[3]	1.500	0.071	0.009	0.7209	0.0017	0.0023
HD 82943d	0.294 ± 0.031	2.137 ± 0.017	[4]	0.278	0.030	0.001	2.0766	0.0167	0.0066
HD 89307b	2.0 ± 0.4	3.34 ± 0.17	[5]	2.074	0.356	0.013	3.3632	0.0619	0.0106
HD 106252b	7.56	2.70	[2]	7.613	0.364	0.147	2.7033	0.0202	0.0259
HD 141937b	9.7	1.52	[6]	9.316	0.306	0.120	1.4877	0.0018	0.0095

Reference: [1] Wright et al. (2009); [2] Perrier et al. (2003); [3] Tan et al. (2013); [4] Baluev & Beaugé (2014); [5] Boisse et al. (2012); [6] Udry et al. (2002).

5 DISCUSSION AND CONCLUSIONS

We investigated the physical state of the six EH stars and their own planets, by employing the method presented by Do Nascimento et al. (2009). In the context of common observations, we added two observational constraints, the lithium abundance $\log N$ (Li) and the rotational period $P_{\rm rot}$, to better determine the fundamental parameters of EH stars and their planets.

We gave the estimations of stellar masses and ages using only the effective temperature $T_{\rm eff}$ and luminosity $L/L_{\odot}$ as observational constraints. The uncertainties in the mass and age are approximately 0.05 $M_{\odot}$ and 4.0 Gyr respectively. As we considered the lithium abundance $\log N$ (Li) and rotational period $P_{\rm rot}$ in our analysis, we obtained more precise determinations. The lithium abundance helped us to minimize the errors in masses and ages to 0.03 $M_{\odot}$ and 3.0 Gyr, respectively. Additionally, we used the rotational period $P_{\rm rot}$ to restrict stellar models based on the former results. The precision has been improved with $\Delta M \sim 0.02\ M_{\odot}$ and $\Delta t \sim 0.5$ Gyr. Furthermore, because of the precise determination of age, we restricted the atmospheric characteristics more strictly than the observations, and positioned the stars more exactly in the H-R diagram. Furthermore, we obtained accurate planetary parameters, i.e., minimum masses $M_2 \sin i$ and orbital semimajor axes a by using previously determined RV measurements and stellar masses.

If we want to completely characterize a system, and obtain accurate properties of the planet, i.e. the mass, radius and density, we need the photometric transit, the RV observations and the properties of the EH star. In the future, we hope to conduct further studies with data from the Gaia mission.

Acknowledgements This work is supported by the National Natural Science Foundation of China (Grant Nos. 10933002, 11273007 and 11273012) and the Fundamental Research Funds for the Central Universities.

References

Angulo, C., Arnould, M., Rayet, M., et al. 1999, Nuclear Physics A, 656, 3
Baluev, R. V., & Beaugé, C. 2014, MNRAS, 439, 673
Baranne, A., Queloz, D., Mayor, M., et al. 1996, A&AS, 119, 373
Batalha, N. M., Rowe, J. F., Bryson, S. T., et al. 2013, ApJS, 204, 24
Baumann, P., Ramírez, I., Meléndez, J., Asplund, M., & Lind, K. 2010, A&A, 519, A87
Bi, S.-L., Basu, S., & Li, L.-H. 2008, ApJ, 673, 1093
Böhm-Vitense, E. 1958, ZAp, 46, 108
Boisse, I., Pepe, F., Perrier, C., et al. 2012, A&A, 545, A55
Bouvier, J., Forestini, M., & Allain, S. 1997, A&A, 326, 1023
Castro, M., Do Nascimento, J. D., Jr., Biazzo, K., Meléndez, J., & de Medeiros, J. R. 2011, A&A, 526, A17
Chaboyer, B., Demarque, P., Guenther, D. B., & Pinsonneault, M. H. 1995, ApJ, 446, 435
Demarque, P., Guenther, D. B., Li, L. H., Mazumdar, A., & Straka, C. W. 2008, Ap&SS, 316, 31
Diego, F., Charalambous, A., Fish, A. C., & Walker, D. D. 1990, in Society of Photo-Optical Instrumentation Engineers (SPIE) Conference Series, 1235, Instrumentation in Astronomy VII, ed. D. L. Crawford, 562
Do Nascimento, J. D., Jr., Castro, M., Meléndez, J., et al. 2009, A&A, 501, 687
Eggenberger, P., Meynet, G., Maeder, A., et al. 2010, A&A, 519, A116
Ferguson, J. W., Alexander, D. R., Allard, F., et al. 2005, ApJ, 623, 585
Ghezzi, L., Cunha, K., Smith, V. V., et al. 2010a, ApJ, 720, 1290
Ghezzi, L., Cunha, K., Smith, V. V., & de la Reza, R. 2010b, ApJ, 724, 154
Grevesse, N., & Sauval, A. J. 1998, Space Sci. Rev., 85, 161
Guenther, D. B., Demarque, P., Kim, Y.-C., & Pinsonneault, M. H. 1992, ApJ, 387, 372
Israelian, G., Santos, N. C., Mayor, M., & Rebolo, R. 2004, A&A, 414, 601
Kaufer, A., Stahl, O., Tubbesing, S., et al. 1999, The Messenger, 95, 8

Kawaler, S. D. 1988, ApJ, 333, 236
Li, L. H., Basu, S., Sofia, S., et al. 2003, ApJ, 591, 1267
Li, T. D., Bi, S. L., Chen, Y. Q., et al. 2012, ApJ, 746, 143
Meléndez, J., Ramírez, I., Casagrande, L., et al. 2010, Ap&SS, 328, 193
Moutou, C., Mayor, M., Lo Curto, G., et al. 2011, A&A, 527, A63
Ofir, A., & Dreizler, S. 2013, A&A, 555, A58
Perrier, C., Sivan, J.-P., Naef, D., et al. 2003, A&A, 410, 1039
Pietrukowicz, P., Minniti, D., Díaz, R. F., et al. 2010, A&A, 509, A4
Pinsonneault, M. H., Kawaler, S. D., & Demarque, P. 1990, ApJS, 74, 501
Pinsonneault, M. H., Deliyannis, C. P., & Demarque, P. 1992, ApJS, 78, 179
Queloz, D., Mayor, M., Weber, L., et al. 2000, A&A, 354, 99
Rogers, F. J., & Nayfonov, A. 2002, ApJ, 576, 1064
Rowe, J. F., Bryson, S. T., Marcy, G. W., et al. 2014, ApJ, 784, 45
Santos, N. C. 2008, New Astron. Rev., 52, 154
Santos, N. C., Delgado Mena, E., Israelian, G., et al. 2010, in IAU Symposium, 268, eds. C. Charbonnel, M. Tosi, F. Primas, & C. Chiappini (Cambridge: Cambridge Univ. Press), 291
Seager, S., & Mallén-Ornelas, G. 2003, ApJ, 585, 1038
Tan, X., Payne, M. J., Lee, M. H., et al. 2013, ApJ, 777, 101
Thoul, A. A., Bahcall, J. N., & Loeb, A. 1994, ApJ, 421, 828
Udry, S., Mayor, M., Naef, D., et al. 2000, A&A, 356, 590
Udry, S., Mayor, M., Naef, D., et al. 2002, A&A, 390, 267
Valenti, J. A., & Fischer, D. A. 2005, ApJS, 159, 141
Vogt, S. S. 1987, PASP, 99, 1214
Vogt, S. S., Allen, S. L., Bigelow, B. C., et al. 1994, in Society of Photo-Optical Instrumentation Engineers (SPIE) Conference Series, 2198, Instrumentation in Astronomy VIII, eds. D. L. Crawford, & E. R. Craine, 362
Vogt, S. S., Marcy, G. W., Butler, R. P., & Apps, K. 2000, ApJ, 536, 902
Winn, J. N. 2010, in Exoplanets, ed. S. Seager (Tucson, AZ: Univ. Arizona Press)
Wright, J. T., Marcy, G. W., Butler, R. P., & Vogt, S. S. 2004, ApJS, 152, 261
Wright, J. T., Upadhyay, S., Marcy, G. W., et al. 2009, ApJ, 693, 1084